



# Programmed Supramolecular Assemblies Using Orthogonal Pairs of Heterodimeric Coiled Coil Peptides

Linhai Jiang, Xiaobing Zuo, Jianping Li, Nathaniel J. Traaseth, and Kent Kirshenbaum\*

In memory of Professor Nadrian Seeman (1945–2021)

**Abstract:** Despite recent progress, it remains challenging to program biomacromolecules to assemble into discrete nanostructures with pre-determined sizes and topologies. We report here a novel strategy to address this challenge. By using two orthogonal pairs of heterodimeric coiled coils as the building blocks, we constructed six discrete supramolecular assemblies, each composed of a prescribed number of coiled coil components. Within these assemblies, different coiled coils were connected via end-to-side covalent linkages strategically pre-installed between the non-complementary pairs. The overall topological features of two highly complex assemblies, a “barbell” and a “quadrilateral” form, were characterized experimentally and were in good agreement to the designs. This work expands the design paradigms for peptide-based discrete supramolecular assemblies and will provide a route for de novo fabrication of functional protein materials.

structured materials with monodisperse sizes are crucial for better quality control and an in-depth understanding of structure-function relationships.

A capping strategy that has emerged recently shows potential as a versatile method to alleviate the challenges of size control.<sup>[6]</sup> Physically mixing the capping component and non-capping building blocks with different molar ratios has been applied to successfully control and narrow the length distribution of peptide nanofibers<sup>[6a]</sup> and nanotubes.<sup>[6b]</sup> In addition to optimizing the molar ratio, it is also important to fine tune the relative strength of three different types of associations. “Heteromeric” associations between non-capping building blocks and capping components are desired, as are “homomeric” associations between the non-capping building blocks. The balance between these two types of association strongly influences the size distribution of the resultant assemblies. A third type of association, homomeric interactions between capping components, are undesired and should be curtailed or eliminated. Precise control of these three types of associations would ideally lead to the formation of discrete molecular assemblies with monodisperse and predictable size. Heterodimeric coiled coils formed by the intermolecular assembly of two complementary polypeptide chains are versatile building blocks and can be considered the simplest case of discrete peptide-based supramolecular assemblies. We considered whether the aforementioned precise control of three different types of associations could be achieved by linking multiple pairs of heterodimeric coiled coils together in strategically designed arrangements, leading to the predictable formation of complex assemblies.

The capabilities for precisely constructing peptide-based supramolecular structures assembled from a defined and pre-determined number of basic building blocks are still largely unrealized to date. There are, however, a few precedents demonstrating some successes for achieving such constructions using heterodimeric coiled coils. The Ghosh group has constructed four-arm dendrimers with monodisperse and pre-determined sizes, in which four identical heterodimeric coiled coils were tethered to a zero-generation poly(amidoamine) dendrimer core.<sup>[7]</sup> The Woolfson group has conjoined two or three heterodimeric coiled coils, thus fashioning rod-like nanostructures with predicted molar masses.<sup>[8]</sup> Utilizing the co-assembly of three different polypeptide chains, the Keating group has designed triangular shaped nanostructures which are composed of three different covalently-connected heterodimeric coiled coils.<sup>[9]</sup> From

## Introduction

Supramolecular assembly of peptides is a bio-inspired and powerful bottom-up approach that has been widely used to create a range of biomaterials with tunable functions for a variety of applications.<sup>[1]</sup> By implementing rational design strategies along with computational algorithms, nanostructured materials with different geometries and dimensions,<sup>[15,16]</sup> such as nanofibers,<sup>[2]</sup> nanotubes,<sup>[3]</sup> nanosheets<sup>[2c,4]</sup> and metal-coordinated assemblies,<sup>[5]</sup> can be fabricated via self-assembly of an individual peptide component or by co-assembly from multiple peptide entities. Although the attractive molecular interactions are always carefully designed to ensure the successful assembly, the termination of these cohesive forces are often not considered thoroughly, leading to difficulties in precisely controlling the size of resultant supramolecular assemblies. Nano-

[\*] L. Jiang, Dr. J. Li, Prof. N. J. Traaseth, Prof. K. Kirshenbaum  
 Chemistry Department, New York University,  
 100 Washington Square E, New York, NY 10003 (USA)  
 E-mail: kk54@nyu.edu

Dr. X. Zuo  
 X-ray Science Division, Argonne National Laboratory  
 Lemont, IL 60439 (USA)

the topological point of view, these precedent works used the termini of heterodimeric coiled coils as the linking points. Such a linking strategy allowed the relatively easy preparation of the linear polypeptide chains using either chemical synthetic methods or biological expression approaches. However, it may cause undesired intramolecular associations which could result in the formation of dead-end monomeric species and also limit the topological space that the final assembled products can access.<sup>[10]</sup>

We envisioned that installing covalent linkages between two or more different heterodimeric coiled coils in an end-to-side (termini-to-side chains) arrangement would be an effective strategy for embellishing peptide-based discrete supramolecular assemblies. In order to achieve the end-to-side linkages, we introduced branch points in the side chains of selected peptide components. The amino acid sequences of a peptide chain that can form coiled coils are often based on tandem seven-residue repeats, denoted (abcdefg)<sub>n</sub>. The residues located at the “f” positions of the heptad repeats are exposed to the solvent and have negligible impact on the coiled coil tertiary structure.<sup>[11]</sup> Thus, these positions were selected as the branch points in order to minimize perturbations to the folding propensities of the original peptide sequences. The undesired intramolecular associations may be largely obviated when two peptides are linked together via a covalent bond between the terminus of one peptide and the side chain of another peptide. This is presumably due to the mis-alignment of the peptide hydrophobic faces that could otherwise drive the formation of the dead-end monomeric species. In addition, the undesired side chain-side chain interactions that may be caused by side-to-side linking would also be largely avoided. The end-to-side linkage strategy would also assist in defining the relative orientation of the heterodimeric coiled coils that will be present within the resultant supramolecular assemblies.<sup>[17,18]</sup> We expected that peptide-based discrete supramolecular assemblies with diverse topologies and predicted sizes could be obtained via a set of end-to-side linking strategies. Herein, we report the implementation of these strategic linkages, leading to the successful construction of several discrete supramolecular assemblies composed of a predicted number of dimeric coiled coil components, with molar masses ranging from  $\approx 20$  kDa to  $\approx 42$  kDa.

## Results and Discussion

Our strategy of constructing discrete supramolecular assemblies relies on a set of peptide sequences that can form orthogonal pairs of heterodimeric coiled coils. Upon searching the literature for a set of such sequences with solved crystal structures, we identified four suitable SYNZIP peptides developed by the Keating group: SYNZIP-1, -2, -5 and -6.<sup>[12]</sup> These four peptides can orthogonally associate with their complementary sequences to form two hetero-specific parallel coiled coil dimers, the SYNZIP-1/SYNZIP-2 dimer (pdb id: 3HE5) and the SYNZIP-5/SYNZIP-6 dimer (pdb id: 3HE4). In this work, we used truncated versions of

these four peptides (Scheme 1), which retained their folding abilities and specificities for orthogonal interactions.

As shown in Scheme 1A, **4A** is a 41-residue long peptide, initially synthesized to contain L-2,3-diaminopropionic acid (Dap) as the C-terminal residue. An azido group was then installed in the side chain of the Dap residue through amide coupling between the side chain amino group and 2-azido acetic acid to complete the synthesis of **4A** (Scheme S1). **4B** is a 40-residue long peptide whose N-terminus was capped by an azidoacetyl group (Scheme 1B). **5A** and **5B** peptides both contain 46 residues. We opted to introduce branch points in the **5A** peptide. **5A1** peptide was obtained by introducing one branch point in **5A** by mutating Lys22 (the “f” position in the third heptad repeat) to Glu22. This subsequently enabled incorporation of an alkyne group through amide coupling between side chain carboxylic acid group of Glu22 and propargylamine (Scheme 1C and S2). We similarly introduced two branch points in **5A** to obtain the **5A2** peptide. In this case, both Asn8 and Lys36 (“f” positions of the first and fifth heptad repeats) of **5A** were mutated to glutamic acids, followed by installing the two side chain alkyne groups in the same way as for **5A1** (Scheme 1D). No mutation or side chain modification was made for **5B** (Scheme 1E). The original sequences of **4B**, **5A1**, **5A2** and **5B** peptides all contain tyrosine residues for accurate concentration determination by measurement of UV absorbance at 280 nm. Similarly, the Lys1 residue originally located at the N-terminus of **4A** peptide was mutated to tryptophan (Scheme 1A). Each single chain peptide was synthesized using standard Fmoc-based solid phase peptide synthesis protocols. The purities were evaluated by analytical HPLC and the chemical identities were confirmed by mass spectrometry. (See Supporting Information for synthetic details and analytical data.)

Based on the design principles, **4A** is complementary with **4B**, while both **5A1** and **5A2** are complementary with **5B** (Scheme 1F–H). Stable dimeric coiled coils can be formed as a single species when the registered pairs are mixed at a 1:1 molar ratio. The hetero-association specificities of each single-chain peptide were confirmed by circular dichroism (CD) spectroscopy. Characteristic CD spectra of well-defined  $\alpha$ -helical secondary structures (minima at 208 nm and 222 nm, respectively) were only observed for the mixtures of registered pairs with 1:1 molar ratios (Figure 1A). Isolated single chain peptides or equimolar mixtures of non-registered pairs showed CD spectra characteristic of weak helical secondary structures with very low thermal stabilities or non-helical secondary structures (Figure 1A, S18 and S19). Based on the temperature-dependent CD studies, the melting temperatures of the coiled coil tertiary structures were estimated at 47 °C for the **4A/4B** mixture, 61 °C for the **5A1/5B** mixture and 63 °C for the **5A2/5B** mixture (Figure 1B). The molar mass estimated by size exclusion chromatography in-line with multi-angle laser scattering (SEC-MALS) verified that the desired dimeric coiled coils were formed from the equimolar mixtures of registered pairs, **4A/4B**, **5A1/5B** and **5A2/5B** (Figure 1C). Computer models of the three dimers were constructed based on the crystal structures of the parent coiled coil

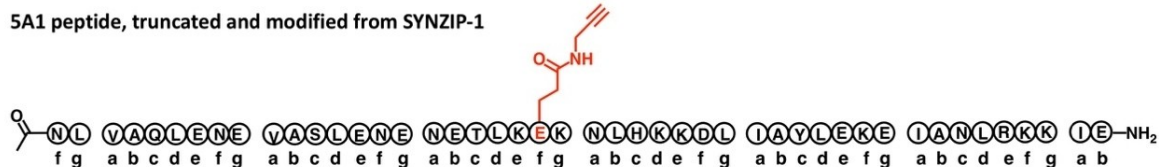
## A. 4A peptide, truncated and modified from SYNZIP-6



## B. 4B peptide, truncated and modified from SYNZIP-5



## C. 5A1 peptide, truncated and modified from SYNZIP-1



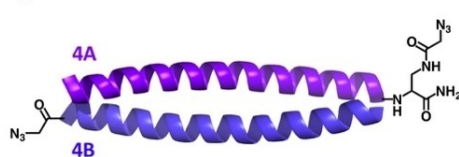
## D. 5A2 peptide, truncated and modified from SYNZIP-1



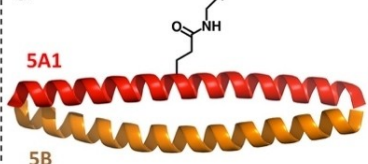
## E. 5B peptide, truncated from SYNZIP-2



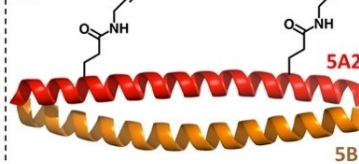
## F.



## G.



## H.



**Scheme 1.** Amino acid sequences of each single chain peptide used in this work: A) **4A**, B) **4B**, C) **5A1**, D) **5A2** and E) **5B**. Heptad repeat patterns are shown below the corresponding sequence. Mutations and side chain modifications are highlighted in red. Cartoon representations of three expected heterodimeric coiled coils: F) **4A/4B** dimer, G) **5A1/5B** dimer and H) **5A2/5B** dimer. Terminal and side chain modifications are highlighted by the corresponding chemical structures.

dimers.<sup>[12]</sup> Excellent agreements were found between the experimental small angle X-ray scattering (SAXS) data and the theoretical SAXS profiles modeled by the FoXS<sup>[13]</sup> computational platform (Figure 1D), suggesting that the overall solution-state structures of each dimeric coiled coil are well-represented by the corresponding model. These results indicate that the terminal and sidechain modifications we introduced have negligible perturbations to the heterodimeric coiled coil tertiary structures formed by the complementary pairs.

We then moved to the synthesis of the peptide conjugates using copper (I) catalyzed azide/alkyne cycloaddition (CuAAC) “click” chemistry. Four different conjugated peptides were successfully prepared through the formation of triazole bonds between the azido groups at the side chain branch points of **5A1** or **5A2** and terminal alkyne groups of **4A** or **4B**, **Con\_5A1-4A**, **Con\_5A1-4B**, **Con\_5A2-(4A)<sub>2</sub>** and **Con\_5A2-(4B)<sub>2</sub>** (Figure 2 and S11–S17). None of these four conjugated peptides showed CD spectra with

mean residue ellipticity higher than 20000 at 222 nm (Figure 2C), indicating that they were all only partially helical and did not form coiled coils. In addition, sigmoidal transitions were not observed by CD for any of these conjugated peptides during the thermal unfolding experiments (Figure S20), further evidencing the absence, as desired, of intramolecular associations which would compete with the designed intermolecular interactions in the presence of the complementary folding partners.

We conceived that barbell shaped supramolecular assembly composed of three dimeric coiled coil components could be constructed by mixing **Con\_5A1-4A**, **Con\_5A1-4B** and **5B** with a 1:1:2 molar ratio (Figure 3C). Prior to constructing the barbell shaped assembly, two intermediate assemblies were constructed, pre-barbell\_A and pre-barbell\_B (Figure 3A and B). The pre-barbell\_A assembly was obtained by preparing a mixture of **Con\_5A1-4A**, **4B** and **5B** peptides with a 1:1:1 molar ratio. Two dimeric coiled coils were expected to be formed within this structure.

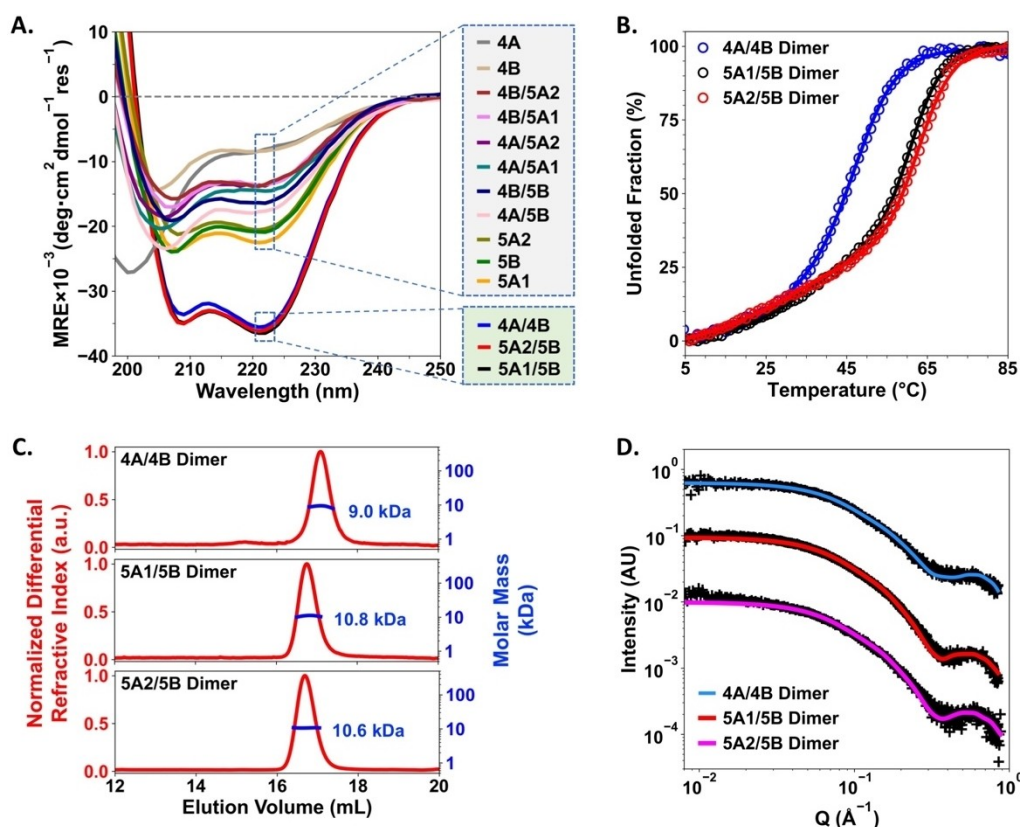


**Figure 1.** A) Circular Dichroism spectra of single chain peptides in isolation, equimolar mixtures of non-registered pairs and equimolar mixtures of registered pairs. The “/” signs indicate equimolar mixtures. B) Thermal denaturation profiles of heterodimeric coiled coils formed by the registered pairs, as monitored by CD at 222 nm. C) SEC-MALS results of the three dimers. Expected molar mass, **4A/4B** dimer: 9.7 kDa; **5A1/5B** dimer: 10.7 kDa; and **5A2/5B** dimer: 10.6 kDa. D) Small-angle X-ray scattering profiles of the **4A/4B**, **5A1/5B** and **5A2/5B** dimers. Experimental data is represented by “+” symbols and theoretical scattering curves of computer models are shown in solid lines. Goodness of fit,  $\chi^2$ (**4A/4B**): 1.04;  $\chi^2$ (**5A1/5B**): 1.12;  $\chi^2$ (**5A2/5B**): 0.96.

Essentially, one **4A/4B** dimer is covalently linked to one **5A1/5B** dimer through a triazole bond formed between the C-terminus of **4A** peptide and the side chain of **5A1** peptide. The CD spectrum of this ternary mixture indicated that well-defined  $\alpha$ -helical secondary structures were adopted by each peptide domain within the coiled coil context (Figure 3D). The coiled coil tertiary structures present within the pre-barbell\_A assembly were more resistant to thermal unfolding than that of isolated **4A/4B** dimer but less resistant than isolated dimeric coiled coils of **5A1/5B** (Figure 3E). This difference in thermal stabilities suggests that each dimeric coiled coil retained its native folding propensity in the context of pre-barbell\_A assembly. The molar mass of pre-barbell\_A assembly was estimated at  $\approx 21$  kDa by SEC-MALS (Figure 3F top), in good agreement to the expected value of 20.6 kDa. The pre-barbell\_B assembly was also successfully constructed by obtaining a mixture of **Con\_5A1-4B**, **4A** and **5B** with 1:1:1 molar ratio. Pre-barbell\_B showed near identical CD spectrum and thermal denaturation profile to that of pre-barbell\_A (Figure 3D and E). The expected molar mass of pre-barbell\_B (also 20.6 kDa) was similarly observed in the SEC-MALS analysis (Figure 3F middle). These results validated our hypothesis that these two intermediate assemblies are composed of one

**4A/4B** and one **5A1/5B** dimeric coiled coil. They differ from each other by having the covalent linkage at different positions with respect to the **4A/4B** dimer: at the C-terminus for pre-barbell\_A and at the N-terminus for pre-barbell\_B.

The success of constructing both pre-barbell\_A and pre-barbell\_B assemblies indicated that the expected hetero-specific intermolecular associations are the dominant driving force in forming these two discrete supramolecular assemblies. The barbell shaped assembly was then constructed by preparing a mixture of **Con\_5A1-4A**, **Con\_5A1-4B** and **5B** with a 1:1:2 molar ratio (Figure 3C). We expected one **4A/4B** and two **5A1/5B** dimeric coiled coils would form within this assembly. A CD spectrum with a strong  $\alpha$ -helical signal was observed for this three-component mixture (Figure 3D). Due to the presence of one additional **5A1/5B** dimer, the overall thermal stabilities of coiled coils tertiary structures presented within this assembly were stronger than that of the two pre-barbell assemblies, and somewhat weaker than that for the isolated **5A1/5B** dimer (Figure 3E). SEC-MALS analysis indicated that a discrete supramolecular assembly with a molar mass  $\approx 32$  kDa was obtained (Figure 3F bottom), in good agreement with the expected molar mass (31.6 kDa) of the barbell shaped assembly composed of two **5A1/5B** dimers and one **4A/4B** dimer.

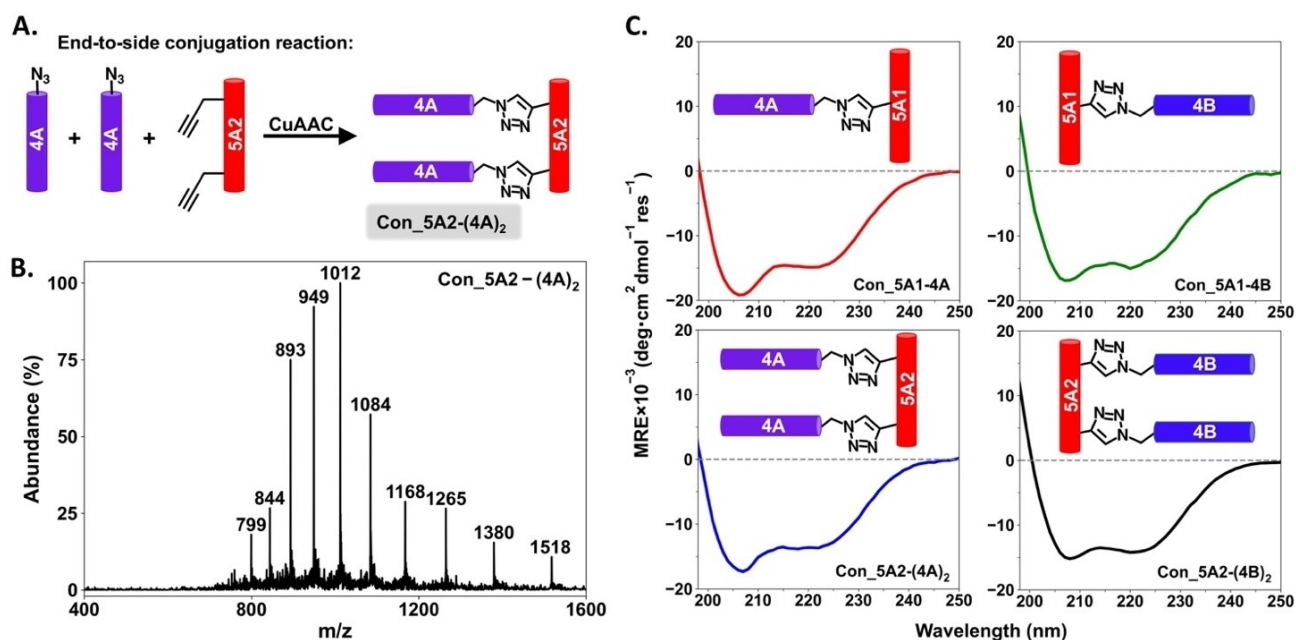


**Figure 2.** A) Synthetic route for conjugating multiple peptide chains together at the branch points of **5A1** or **5A2** via CuAAC click chemistry, as exemplified for **Con\_5A2-(4A)<sub>2</sub>**. B) Mass spectrometry data for **Con\_5A2-(4A)<sub>2</sub>**. Expected mass:  $[M+H]^+/1 = 15171$ ,  $[M+10H]^{10+}/10 = 1518$ ,  $[M+11H]^{11+}/11 = 1380$ ,  $[M+12H]^{12+}/12 = 1265$ ,  $[M+13H]^{13+}/13 = 1168$ ,  $[M+14H]^{14+}/14 = 1085$ ,  $[M+15H]^{15+}/15 = 1012$ ,  $[M+16H]^{16+}/16 = 949$ ,  $[M+17H]^{17+}/17 = 893$ ,  $[M+18H]^{18+}/18 = 844$ ,  $[M+19H]^{19+}/19 = 799$ . C) CD spectra of the four different conjugated peptides, **Con\_5A1-4A** (upper left), **Con\_5A1-4B** (upper right), **Con\_5A2-(4A)<sub>2</sub>** (lower left) and **Con\_5A2-(4B)<sub>2</sub>** (lower right). The subscripts indicate the number of peptide units. Schematic representation of each conjugated peptide is inserted to the corresponding CD spectrum. The weak signals at 208 nm and 222 nm indicate the expected absence of coiled coil assemblies.

We further conceived that replacing **Con\_5A1-4A** and **Con\_5A1-4B** in the barbell shaped assembly by **Con\_5A2-(4A)<sub>2</sub>** and **Con\_5A2-(4B)<sub>2</sub>**, respectively, would lead to the formation of quadrilateral shaped structure in which each side is established by a dimeric coiled coil component (Figure 4C). Similar to the construction of the pre-barbell assemblies, two pre-quadrilateral assemblies were also constructed prior to attempting the construction of the quadrilateral shaped assembly. Pre-quadrilateral\_A assembly was obtained by creating a mixture of **Con\_5A2-(4A)<sub>2</sub>**, **4B** and **5B** with a 1:2:1 molar ratio (Figure 4A). Maintaining the same molar ratio but replacing the **Con\_5A2-(4A)<sub>2</sub>** and **4B** with **Con\_5A2-(4B)<sub>2</sub>** and **4A**, respectively, resulted in the formation of the pre-quadrilateral\_B assembly (Figure 4B). The CD spectra of these two three-component mixtures generated strong characteristic  $\alpha$ -helical signals, indicating well-defined  $\alpha$ -helical secondary structures were formed for both pre-quadrilateral assemblies (Figure 4D). Upon heating, these two pre-quadrilateral assemblies unfolded less readily than isolated **4A/4B** dimer but more readily than **5A2/5B** dimer (Figure 4E). The expected molar mass determined by SEC-MALS analysis further confirmed that both of these two pre-quadrilateral assemblies contain two **4A/4B** dimers and one **5A2/5B** dimer (Figure 4F **top** and **middle**, expected mass: 31.6 kDa for both pre-quadrilateral assemblies, observed mass:  $\approx 30$  kDa for pre-quadrilateral\_A assembly and  $\approx 32$  kDa for pre-quadrilateral\_B assembly).

The construction of the quadrilateral shaped assembly was then carried out by preparing a mixture containing **Con\_5A2-(4A)<sub>2</sub>**, **Con\_5A2-(4B)<sub>2</sub>** and **5B** with a 1:1:2 molar ratio (Figure 4C). As expected, CD spectra consistent with well-defined  $\alpha$ -helical secondary structures were observed for this three-component mixture (Figure 4D). In comparison to the two pre-quadrilateral assemblies, the thermal stability of quadrilateral shaped assembly increased slightly but was still weaker than the isolated **5A2/5B** dimer (Figure 4E). The expected molar mass was also observed in the SEC-MALS analysis for the quadrilateral shaped assembly (Figure 4F **bottom**, expected mass: 42.6 kDa and observed mass:  $\approx 44$  kDa).

The results from CD and SEC-MALS studies clearly indicated that discrete supramolecular assemblies with a pre-determined number of coiled coil components were successfully constructed. We further evaluated the structural features of the barbell and quadrilateral shaped assemblies by using Small Angle X-ray Scattering (Figure 5A). Guinier analysis of the SAXS data shows that these two assemblies have a similar radius of gyration ( $R_g$ ),  $\approx 31$  Å for barbell shaped assembly and  $\approx 33$  Å for quadrilateral shaped assembly (Figure S33B and S34B). Such similarity was also found for the  $R_g$  estimated from pair-distance distribution ( $P(r)$ ) functions,  $\approx 34$  Å for barbell shaped assembly and  $\approx 36$  Å for quadrilateral shaped assembly (Figure 5B). The  $P(r)$  functions of these two assemblies showed similar asymmetric profiles, while the maximum dimension ( $d_{max}$ ) of

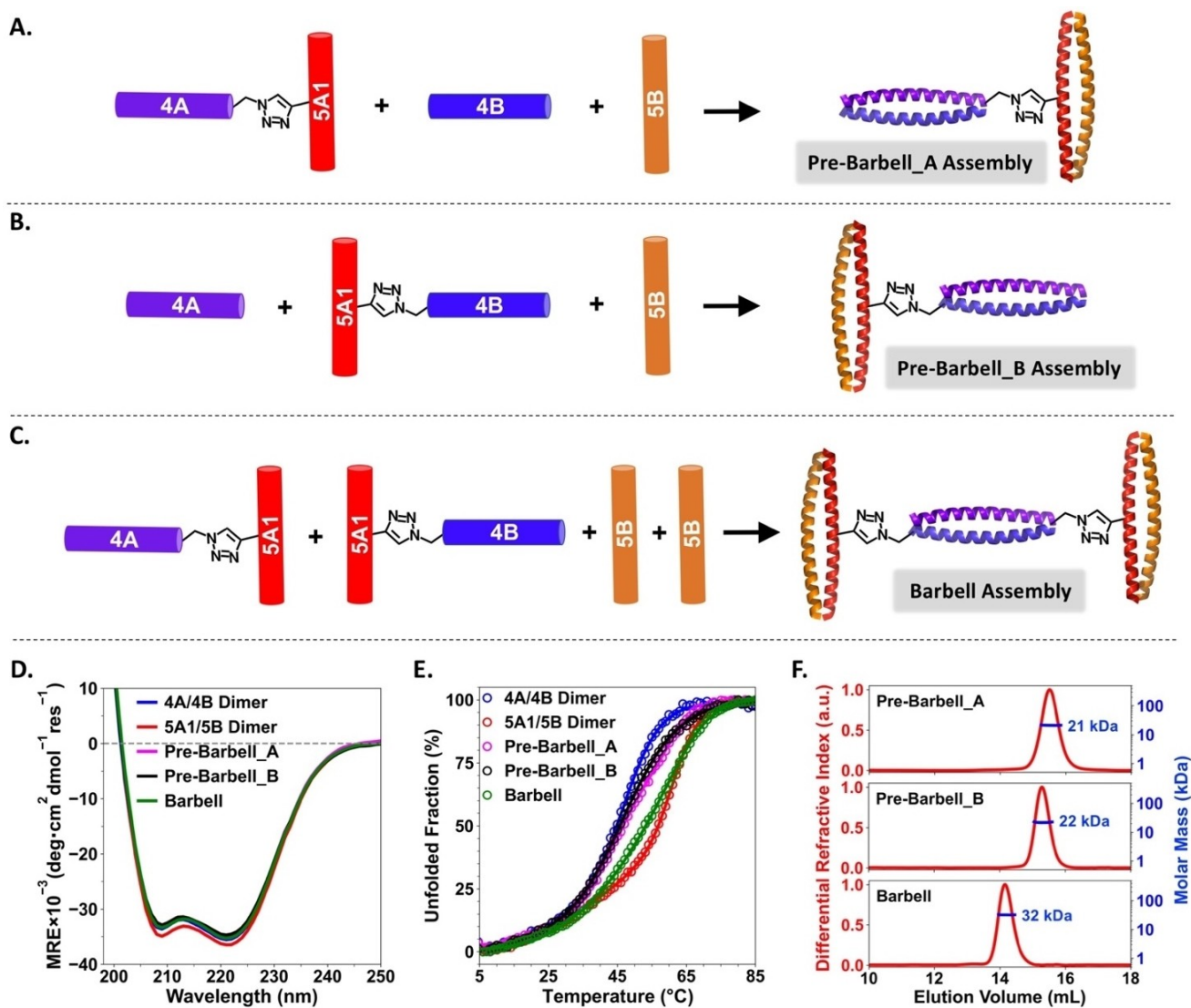


**Figure 3.** Preparation routes of pre-barbell\_A (A), pre-barbell\_B (B) and barbell shaped (C) assemblies. Comparison of CD spectra (D) and thermal denaturation profiles (E) between the dimeric building blocks (4A/4B and 5A1/5B dimers) and supramolecular assemblies in the barbell series. F) SEC-MALS results of the three assemblies. Expected molar mass, pre-barbell\_A assembly: 20.6 kDa; pre-barbell\_B assembly: 20.6 kDa and barbell shaped assembly: 31.6 kDa.

quadrilateral assembly was estimated to be  $\approx 137$  Å, 12 Å longer than that for the barbell assembly ( $d_{\max} \approx 125$  Å).

In order to extract more structural insights from the experimental SAXS data, molecular dynamics (MD) simulations were performed to generate computer models that could illuminate the experimental SAXS data. (See Supporting Information for the simulation details.) Good agreements were found between the experimental SAXS profile and those calculated from MD models by using the FoXS package<sup>[13]</sup> (Figure 5A, C and D). The overall structure of barbell shaped assembly resembles a distorted letter “H” form. The triazole linkers that connect one 4A/4B dimer and two 5A1/5B dimers in the barbell shaped assembly are not rigid by design. As a result, the extent of lateral distortion is somewhat variable. The experimental SAXS profile of barbell assembly could be well-fit by different MD

models with different relative positions of one dimeric coiled coil component with respect to the other two (Figure 6A and B). The overall shapes of the MD models that correspond to the experimental SAXS data of quadrilateral assembly resemble parallelograms. Presumably due to the fact that the two 5A2/5B dimeric coiled coils were connected by two 4A/4B dimeric coiled coils, the overall structure of the quadrilateral shaped assembly is less flexible than that of barbell shaped assembly, for which two 5A1/5B dimers are connected by a single 4A/4B dimer (Figure 6, S35–S38, Animation S1–S2 and Supporting Information pse files).

The structural features of the quadrilateral assembly were further investigated by transmission electron microscopy (TEM) using the negative staining method. We observed protein particles with consistent apparent diameters  $\approx 13$  nm (Figure 7 and S39). In addition, the expected

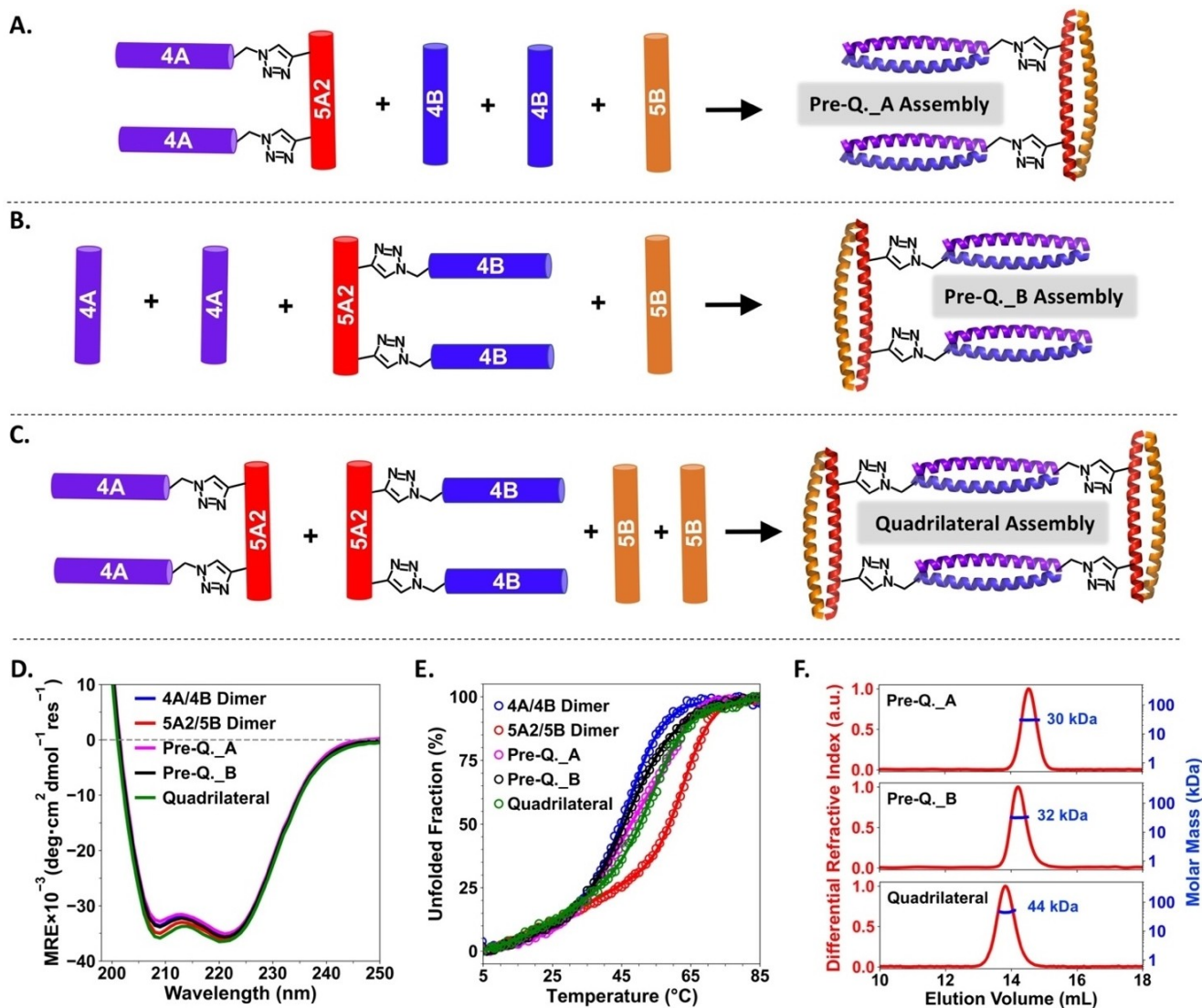


**Figure 4.** Preparation routes for pre-quadrilateral\_A (A), pre-quadrilateral\_B (B) and quadrilateral shaped (C) assemblies. Comparison of CD spectra (D) and thermal denaturation profiles (E) between the dimeric building blocks (4A/4B and 5A2/5B dimers) and the supramolecular assemblies in the quadrilateral series. F) SEC-MALS results of the three assemblies in the quadrilateral series. Expected molar mass, pre-quadrilateral\_A assembly: 31.6 kDa; pre-quadrilateral\_B assembly: 31.6 kDa and quadrilateral shaped assembly: 42.6 kDa.

pore structure exhibited by the quadrilateral shaped assembly were also observed for several particles suitably oriented on the TEM grid (red circles in Figure 7).

In comparison to prior studies in which discrete supramolecular assemblies were obtained after empirical evaluation,<sup>[14]</sup> the strategy reported in this work allows us to pre-determine the size and approximate topologies of the resultant supramolecular assemblies. Notably, supramolecular assemblies composed of four dimeric coiled coil components have also been constructed by the Woolfson group.<sup>[14f]</sup> Only one pair of peptides that form heterodimeric coiled coils were used in their study. The two complementary peptide sequences were spaced by a (glycine-asparagine)<sub>n</sub> linker within one linear peptide chain. Discrete supramolecular assemblies with an oligomeric state of four were obtained only when n equaled to

three and after an annealing process. Larger sized aggregates were obtained when n was less than three. Smaller nanoscale objects composed of three or two dimeric coiled coil components were formed when n was larger than three. Prior to the empirical experimentation, it may not have been feasible to anticipate reliably the relationships between the linker length and the size/heterogeneities of the resultant supramolecular assemblies.

Among the six discrete supramolecular assemblies constructed in this work, the quadrilateral shaped assembly is the only one that has the geometry of an enclosed shape. For this reason, when we have a ternary mixture of **Con\_5A2-(4A)<sub>2</sub>**, **Con\_5A2-(4B)<sub>2</sub>** and **5B** with a 1:1:2 molar ratio, it is possible that larger sized species could form in competition with the desired formation of discrete quadrilateral shaped assembly. Assuming the two **4A/4B** dimeric

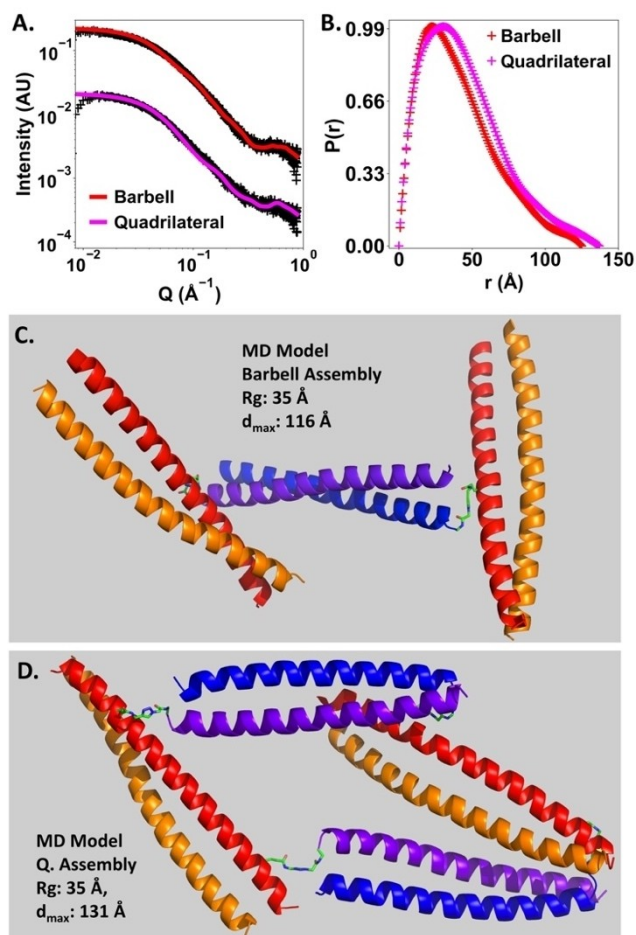


**Figure 5.** A) Small-angle X-ray scattering (SAXS) analysis of the barbell and quadrilateral shaped assemblies. (+) Experimental data, solid line: theoretical curve calculated by FoXS for the representative MD models shown in (C) and (D). Goodness of fit,  $\chi^2$ (barbell): 0.93;  $\chi^2$ (quadrilateral): 0.87. B) Pair distance distribution functions of the barbell and quadrilateral shaped assemblies. Structural parameters derived from  $P(r)$  functions,  $R_g$ (barbell): 33.7 Å,  $d_{max}$ (barbell): 125 Å.  $R_g$ (quadrilateral): 36.5 Å,  $d_{max}$ (quadrilateral): 137 Å.

coiled coils of the quadrilateral shaped assembly formed sequentially, after one **4A/4B** dimeric coiled coil was formed between one **Con\_5A2-(4A)<sub>2</sub>** and one **Con\_5A2-(4B)<sub>2</sub>**, there would be two possible pathways for the remaining **4A** and **4B** peptides to assemble with the complementary sequences. First, the remaining **4A** and **4B** chains could pair together to form another **4A/4B** dimeric coiled coil which would constitute the other edge of the quadrilateral shaped assembly (Figure 8A). Second, it is also possible for the remaining **4A** and **4B** chains to pair with complementary sequences from other **Con\_5A2-(4A)<sub>2</sub>** and **Con\_5A2-(4B)<sub>2</sub>** components (Figure 8B). Fibrillar assemblies with uncontrolled length could result from the second pathway. We considered that the probability of the first pathway would be much higher because the effective local concentrations of **4A** and **4B** components are much higher than the overall concentrations of conjugated peptides in our experiments. Due to the end-to-side conjugation strategy, the relative

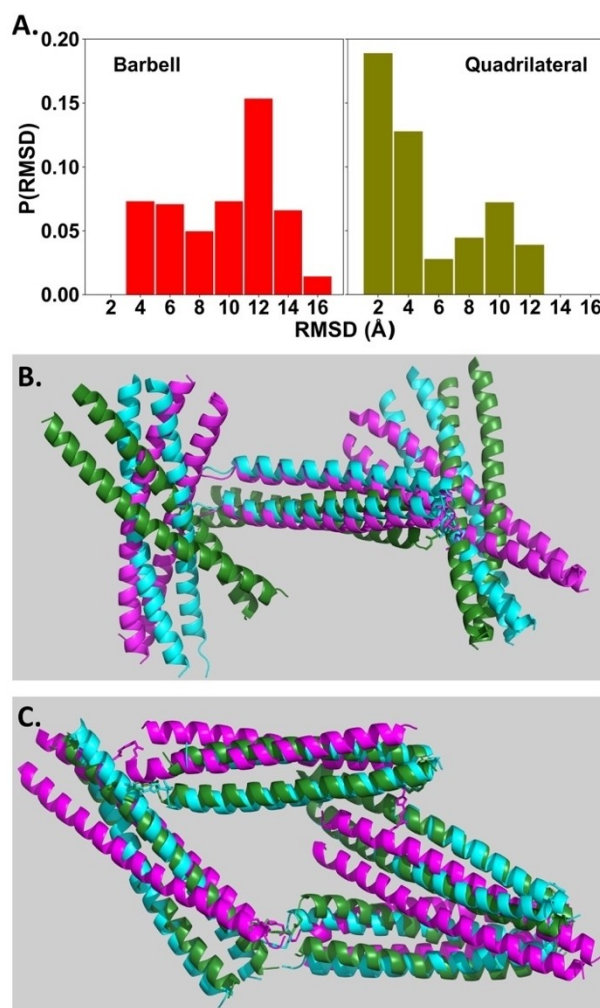


**Figure 6.** A) Histogram plots of  $C\alpha$ -RMSD values of all Molecular Dynamics models that could fit the experimental SAXS data of barbell (left) and quadrilateral (right) shaped assemblies. Three different models of barbell (B) and quadrilateral (C) shaped assemblies are overlaid. The cyan-coloured model was used as the reference for calculating  $C\alpha$ -RMSD values. The green- and magenta-coloured representative models show the median and largest  $C\alpha$ -RMSD values, respectively. (See Figure S35–S38, Amination S1 and S2 and supplementary pse files for more details of analysis.)

orientation of the remaining **4A** and **4B** were also pre-aligned in a form close to parallel alignment. This alignment would further facilitate their hetero association and lead to the formation of a quadrilateral shaped assembly. In addition, the hetero-specific associations between **4A** and **4B** components are orthogonal to that between **5A2** and **5B** components which constitute the other two sides of the quadrilateral assemblies. As a consequence, the predicted quadrilateral shaped assemblies are likely favored relative to other possible assemblies.

Annealing is a commonly used technique during supramolecular assembly processes to circumvent paths leading to undesired thermodynamic states. For instance, the Keating group applied a rational annealing process composed of heating, slow cooling and fast cooling to

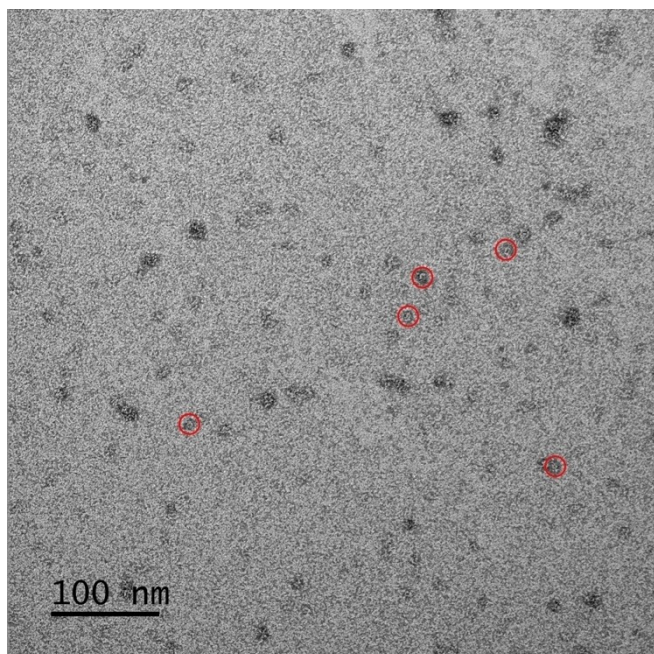


**Figure 7.** TEM image of the quadrilateral shaped assembly. Red circles highlight five single particles with visible pore structures. See Figure S39 for other TEM images.

generate the desired protein nanotriangles and avoid the formation of undesired side products.<sup>[9]</sup> Annealing was not required to obtain the six discrete supramolecular assemblies constructed in this work, indicating the absence of strong competing molecular interactions that would otherwise interfere with the formation of the desired discrete supramolecular assemblies.

## Conclusion

By using two pairs of orthogonally interacting peptides and installing covalent triazole linkages between the non-complementary pairs in a strategic end-to-side arrangement, we constructed six discrete supramolecular assemblies with a pre-determined number of coiled coil components. All coiled coil components retained their native folding abilities and orthogonal dimer-interaction specificity in the context of the supramolecular structures. Hetero specific interactions between complementary peptide chains are the foundation of this work. The molar mass and approximate topologies of the resultant supramolecular assemblies are directed by the number and the location of the branch points we introduced to the parent **5A** peptide, and by the stoichiometry of the multi-component mixture.

From the design point of view, our strategy is highly expandable and customizable. For instance, one-dimensional assemblies with pre-determined length could be constructed when branch points are also introduced to **5B** peptide. Furthermore, our design is compatible with peptides that can form higher order oligomeric assemblies by using different coiled coil structures. In this fashion, replacing

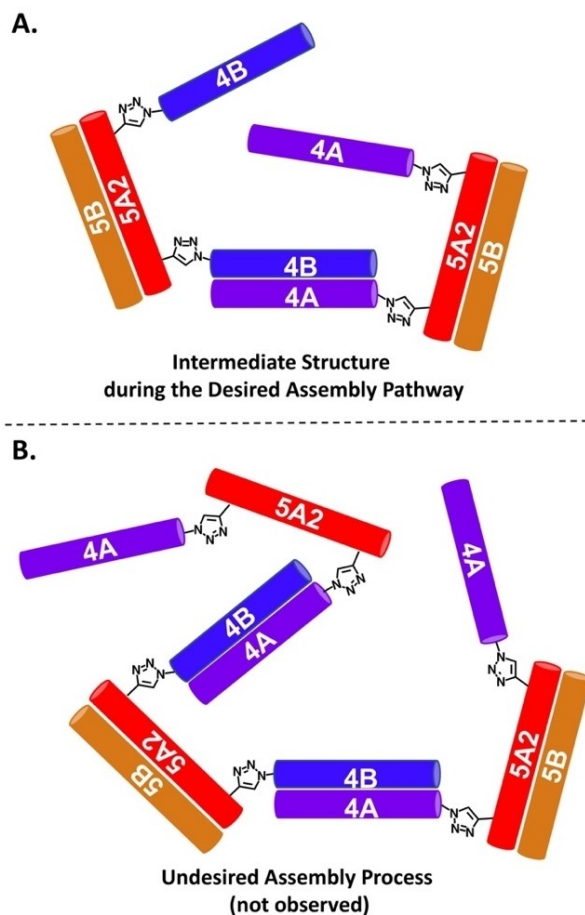


**Figure 8.** A) Plausible intermediate state during formation of the desired quadrilateral shaped assembly. B) Hypothetical intermediate state with low probability.

**5A1/5B** or **5A2/5B** dimers may allow construction of other two- or three-dimensional structures with pre-determined sizes and tunable structural properties. The interior pores of the quadrilateral assemblies may be particularly suitable for functionalization and/or sequestration of ligands in future efforts to develop applications of these assemblies.

Our design paradigm is not limited to coiled coil peptides—collagen mimetic peptides that form homo or hetero collagen triple helices could also be utilized as alternatives to **5A1/5B** or **5A2/5B** dimers. In addition, the N- and C-termini of the **5A1/5B** dimer, **5A2/5B** dimer and their potential replacements are amenable to alternative functionalization. Thus, we believe the strategy reported in this work will have broad potential in constructing customized supramolecular assemblies for a wide range of envisioned applications.

## Acknowledgements

This study was supported by award CHE-2002890 from the National Science Foundation (NSF). L.J. would like to gratefully acknowledge the New York University Chemistry Department for the Margaret and Herman Sokol Fellow-

ship. N.J.T. acknowledges support from NIH R01AI108889. The authors would like to thank Dr. Shahid Khan for the assistance on SEC purifications. Dr. Jia Ma from the Chemistry Department of Columbia University is greatly appreciated for the assistance on performing the SEC-MALS analysis. This work was supported in part through the NYU IT High Performance Computing resources, services, and staff expertise. Joseph Sall, Dr. Feng-Xia (Alice) Liang and Dr. William J. Rice from NYU School of Medicine are greatly acknowledged for assistance with TEM imaging. The authors acknowledge the contribution of James Eastwood for assistance with this manuscript and Prof. Vikas Nanda (Rutgers University) for helpful discussions. The Circular Dichroism Spectropolarimeter used in this work was acquired through the support of New York University. SAXS measurements were performed at Beamline 12-ID-B of the Advanced Photon Source, a U.S. Department of Energy (DOE) Office of Science User Facility operated for the DOE Office of Science by Argonne National Laboratory under Contract No. DE-AC02-06CH11357.

### Conflict of Interest

The authors declare no conflict of interest.

### Data Availability Statement

The data that support the findings of this study are available from the corresponding author upon reasonable request.

**Keywords:**  $\alpha$ -Helices · Coiled Coils · Heterodimers · Nanostructures · Peptides · Supramolecular Assemblies

- [1] a) E. De Santis, M. G. Ryadnov, *Chem. Soc. Rev.* **2015**, *44*, 8288–8300; b) P. Makam, E. Gazit, *Chem. Soc. Rev.* **2018**, *47*, 3406–3420; c) B. J. Kim, D. Yang, B. Xu, *Trends Chem.* **2020**, *2*, 71–83; d) A. L. Boyle, D. N. Woolfson, *Chem. Soc. Rev.* **2011**, *40*, 4295–4306; e) D. M. Raymond, B. L. Nilsson, *Chem. Soc. Rev.* **2018**, *47*, 3659–3720.
- [2] a) A. N. Moore, J. D. Hartgerink, *Acc. Chem. Res.* **2017**, *50*, 714–722; b) C. A. Hauser, S. Zhang, *Chem. Soc. Rev.* **2010**, *39*, 2780–2790; c) A. S. Parmar, J. K. James, D. R. Grisham, D. H. Pike, V. Nanda, *J. Am. Chem. Soc.* **2016**, *138*, 4362–4367.
- [3] a) M. R. Ghadiri, J. R. Granja, R. A. Milligan, D. E. McRee, N. Khazanovich, *Nature* **1993**, *366*, 324–327; b) X. Gao, H. Matsui, *Adv. Mater.* **2005**, *17*, 2037–2050; c) C. Valéry, F. Artzner, M. Paternostre, *Soft Matter* **2011**, *7*, 9583–9594; d) J. Y. Rho, H. Cox, E. D. H. Mansfield, S. H. Ellacott, R. Peltier, J. C. Brendel, M. Hartlieb, T. A. Waigh, S. Perrier, *Nat. Commun.* **2019**, *10*, 4708; e) N. C. Burgess, T. H. Sharp, F. Thomas, C. W. Wood, A. R. Thomson, N. R. Zaccai, R. L. Brady, L. C. Serpell, D. N. Woolfson, *J. Am. Chem. Soc.* **2015**, *137*, 10554–10562.
- [4] a) T. Jiang, C. Xu, X. Zuo, V. P. Conticello, *Angew. Chem. Int. Ed.* **2014**, *53*, 8367–8371; *Angew. Chem.* **2014**, *126*, 8507–8511; b) B. Dai, D. Li, W. Xi, F. Luo, X. Zhang, M. Zou, M. Cao, J. Hu, W. Wang, G. Wei, Y. Zhang, C. Liu, *Proc. Natl. Acad. Sci. USA* **2015**, *112*, 2996–3001.
- [5] a) N. A. Tavenor, M. J. Murnin, W. S. Horne, *J. Am. Chem. Soc.* **2017**, *139*, 2212–2215; b) K. A. Scheib, N. A. Tavenor, M. J. Lawless, S. Saxena, W. S. Horne, *Chem. Commun.* **2019**, *55*, 7752–7755.
- [6] a) C. N. Fries, Y. Wu, S. H. Kelly, M. Wolf, N. L. Votaw, S. Zauscher, J. H. Collier, *Adv. Mater.* **2020**, *32*, 2003310; b) L. Adler-Abramovich, P. Marco, Z. A. Arnon, R. C. G. Creasey, T. C. T. Michaels, A. Levin, D. J. Scurr, C. J. Roberts, T. P. J. Knowles, S. J. B. Tendler, E. Gazit, *ACS Nano* **2016**, *10*, 7436–7442.
- [7] M. Zhou, D. Bentley, I. Ghosh, *J. Am. Chem. Soc.* **2004**, *126*, 734–735.
- [8] E. H. C. Bromley, R. B. Sessions, A. R. Thomson, D. N. Woolfson, *J. Am. Chem. Soc.* **2009**, *131*, 928–930.
- [9] W. M. Park, M. Bedewy, K. K. Berggren, A. E. Keating, *Sci. Rep.* **2017**, *7*, 10577.
- [10] M. Zhou, I. Ghosh, *Org. Lett.* **2004**, *6*, 3561–3564.
- [11] a) G. Grigoryan, A. E. Keating, *Curr. Opin. Struct. Biol.* **2008**, *18*, 477–483; b) D. N. Woolfson, *Adv. Protein Chem.* **2005**, *70*, 79–112.
- [12] A. W. Reinke, R. A. Grant, A. E. Keating, *J. Am. Chem. Soc.* **2010**, *132*, 6025–6031.
- [13] a) D. Schneidman-Duhovny, M. Hammel, J. A. Tainer, A. Sali, *Biophys. J.* **2013**, *105*, 962–974; b) D. Schneidman-Duhovny, M. Hammel, J. A. Tainer, A. Sali, *Nucleic Acids Res.* **2016**, *44*, W424–W429.
- [14] a) L. Jiang, D. Xu, K. E. Namitz, M. S. Cosgrove, R. Lund, H. Dong, *Small* **2016**, *12*, 5126–5131; b) L. Jiang, S. Yang, R. Lund, H. Dong, *Biomater. Sci.* **2018**, *6*, 272–279; c) S. Raman, G. Machaidze, A. Lustig, U. Aebi, P. Burkhard, *Nanomedicine* **2006**, *2*, 95–102; d) F. Boato, R. M. Thomas, A. Ghasparian, A. Freund-Renard, K. Moehle, J. A. Robinson, *Angew. Chem. Int. Ed.* **2007**, *46*, 9015–9018; *Angew. Chem.* **2007**, *119*, 9173–9176; e) J. E. Noble, E. De Santis, J. Ravi, B. Lamarre, V. Castelletto, J. Mantell, S. Ray, M. G. Ryadnov, *J. Am. Chem. Soc.* **2016**, *138*, 12202–12210; f) A. L. Boyle, E. H. Bromley, G. J. Bartlett, R. B. Sessions, T. H. Sharp, C. L. Williams, P. M. Curmi, N. R. Forde, H. Linke, D. N. Woolfson, *J. Am. Chem. Soc.* **2012**, *134*, 15457–15467.
- [15] N. J. Sinha, M. G. Langenstein, D. J. Pochan, C. J. Kloxin, J. G. Saven, *Chem. Rev.* **2021**, *121*, 13915–13935.
- [16] S. Lou, X. Wang, Z. Yu, L. Shi, *Adv. Sci.* **2019**, *6*, 1802043.
- [17] M. G. Ryadnov, D. N. Woolfson, *Angew. Chem. Int. Ed.* **2003**, *42*, 3021–3023.
- [18] X. Yuan, L. Jiang, W. Chen, B. Song, W. Chen, X. Zuo, X. Sun, X. Li, K. Kirshenbaum, S. Luo, H. Dong, *Chem. Commun.* **2020**, *56*, 7128–7131.

Manuscript received: February 3, 2022

Accepted manuscript online: April 12, 2022

Version of record online: May 5, 2022